Phyton-
International Journal of
Experimental Botany

Tech Science Press

DOI: 10.32604/phyton.2023.027046

ARTICLE

Proteomic Analyses of Three Inflorescence Styles of Castor (*Ricinus communis* L.) at Different Developmental Stages

Xue Lei[1,#], Yong Zhao[2,#], Rui Luo[1], Mingda Yin[1], Yanpeng Wen[1], Zhiyan Wang[1], Xuemei Hu[1] and Fenglan Huang[1,3,4,5,*]

[1]College of Life Science and Food Engineering, Inner Mongolia Minzu University, Tongliao, 028043, China

[2]Laboratory of Genetics, Baicheng Normal University, Baicheng, 137000, China

[3]Key Laboratory of Castor Breeding of the State Ethnic Affairs Commission, Tongliao, 028043, China

[4]Inner Mongolia Key Laboratory of Castor Breeding, Tongliao, 028043, China

[5]Inner Mongolia Engineering Research Center of Industrial Technology Innovation of Castor, Tongliao, 028043, China

*Corresponding Author: Fenglan Huang. Email: huangfenglan@imun.edu.cn

[#]These authors contributed equally to this work

Received: 11 October 2022 Accepted: 23 December 2022

ABSTRACT

Castor (*Ricinus communis* L.) is one of ten oil crops in the world and has complex inflorescence styles. Generally, castor has three inflorescence types: single female inflorescence (SiFF), standard female inflorescence (StFF) and bisexual inflorescence (BF). StFF is realized as a restorer line and as a maintainer line, which was applied to castor hybrid breeding. However, the developmental mechanism of the three inflorescences is not clear. Therefore, we used proteomic techniques to analyze different inflorescence styles. A total of 72 diferentially abundant protein species (DAPs) were detected. These DAPs are primarily involved in carbon and energy metabolism and carbon fixation in the photosynthetic organism pathway. The results showed that DAPs are involved in photosynthesis to control the distribution of imported carbohydrates and exported photoassimilates and thus affect the inflorescence development of castor. In addition, these DAPs are also involved in cysteine and methionine metabolism. Quantitative real-time PCR (qRT-PCR) results demonstrated that the proteomics data collected in this study were reliable. Our findings indicate that the carbon cycle and amino acid metabolism influence the inflorescence development of castor.

KEYWORDS

Ricinus communis L.; inflorescence; proteomics

1 Introduction

Castor bean (*Ricinus communis* L.) originated in Africa is a renewable industrial oil crop as an annual or perennial crop [1]. Because castor oil contains special fatty acids that crack to form sebacic acid, castor bean has become a raw material for nylon, high-grade lubricants, cold-resistant plastics and paints for the cosmetics industry [2]. In addition, *R. communis* has been used as a potential source of biodiesel feedstock [2]. Accordingly, castor has been cultivated in many countries, such as India, China and Brazil.

R. communis has a complex inflorescence system, which causes difficulties in traditional castor production and castor breeding [3]. Generally, castor plants contain separate male and female flowers on the same individual. In addition, the female inflorescence of castor shows only female flowers, and a castor monoecious inflorescence bears both female and male flowers [4–6]. Now, the Lm female line of castor cultivated by the Tongliao Agricultural Science Institution can be used for the hybridization of species and strains as a male sterility line or maintainer line. Thus, the Lm female line can basically solve the technological problem of castor production in China. For the Lm female line, there are three inflorescence types, including single female inflorescence (SiFF), standard female inflorescence (StFF) and bisexual inflorescence (BF). A microscopic comparison of terminal bud development of three Lm female line inflorescence types showed that flower bud differentiation occurred in the 5~6-leaf stage and that willow-shaped functional leaves began to appear in the 7-leaf stage [7]. Generally, the 4 euphylla stage is the vegetative growth period of castor inflorescence, and the 5 euphylla stage is the floral bud differentiation period of castor inflorescence. The sex of castor was determined by the inflorescence type of the main stem heading stage and second-level branching state. Accordingly, three inflorescence types were selected for proteome analysis at different developmental stages, including the 4 euphylla stage, 5 euphylla stage, main stem heading stage and second-level branching state.

Plant developmental biology focuses less on gender development than other fields of study, despite their theoretical and practical importance [8]. The sex expression of castor may be controlled by many factors, including heredity, environment, development, etc. For example, high temperature can induce the male development of plants [9]. Season, temperature, photoperiod, light, age of the plant, nutrient level, vegetative activity, pruning, and plant hormones are examples of environmental and intrinsic elements that have an impact on the expression of sex in castor [6,10–12]. Despite significant advancements, the aforementioned ideas remain vulnerable in the lack of cytological data, and little is known about the molecular mechanisms underlying sex variation and the genes responsible for sex expression in castor. Transcriptome analysis of the apical and raceme stages of female and hermaphroditic lines showed that more genes were expressed at the raceme formation and infant raceme stages than at the early leaf bud stage [13].

In this study, our main objective was to identify candidate proteins in different castor inflorescence types. The results will lay the foundation for the study of the mechanism of inflorescence development in castor.

2 Materials and Methods

2.1 Sample Collection

Three samples were collected from the Tongliao Agricultural Science Research Institute experimental field (latitude 43.6 N, longitude 122.3 E). The fresh inflorescence of aLmAB2 (*R. communis* L.) were randomly collected at each location, immediately frozen in liquid nitrogen and stored at −80°C until analysis. All aLmAB2 castor seeds were provided by the Tongliao Agricultural Science Research Institute. The aLmAB2 line has three types of inflorescence including the SiFF, StFF and BF. In this study, at the 4 euphylla stage, 5 euphylla stage, primary stem-heading stage and second-level branching stage, SiFF, StFF and BF were harvested. Each group was conducted with three independent biological replicates.

2.2 Protein Extraction

Total protein was extracted from three inflorescences, including SiFF, StFF and BF. The inflorescence was ground to a fine powder in liquid nitrogen with a mortar and pestle, and then suspended in 10 mL Tris saturated phenol and 10 mL extraction solution containing 0.1 M Tris-HCl, 10 mM EDTA, 0.4% 2-ME and 0.9 M sucrose. The mixture was centrifuged at 10,000 × g at 4°C for 20 min, and the supernatant was removed. Then, 10 mL ammonium acetate methanol solution (0.1 M) was added to the precipitate, and

the mixture was stored at −20°C for 10 min. Then, the mixture was centrifuged at 20,000 × g at 4°C for 20 min, and the supernatant was discarded twice. The pellets were then freeze-dried and stored at −80°C. The protein powder was solubilized in lysis buffer [7 M urea, 2 M thiourea, 4% (w/v) CHAPS, 40 mM DTT, 2% (v/v) pharmalyte (pH 4–7) and 4% (v/v) protease inhibitor] and shaken for 2 h at room temperature, and the insoluble tissue was removed by centrifugation at 30,000 × g and 4°C for 30 min. The subsequent supernatant was collected. The protein content was assayed using a 2D Quant kit (GE Healthcare). The samples were frozen in liquid nitrogen and stored at −80°C until further use.

2.3 Gel Electrophoresis and Gel Staining

Two-dimensional electrophoresis (2-DE) was carried out according to the method of Granier [14]. A 1,200 μg protein sample was added to 450 μL rehydration solution [7 M urea, 2 M thiourea, 2% (w/v) CHAPS, 40 mM DTT and 0.5% (v/v) pH 4–7 IPG buffer] and loaded onto Immobiline Dry Strips (pH 4–7 IPG strips, 24 cm) (GE Healthcare Bio-Sciences Corp., Piscataway, NJ, USA) overnight. After overnight rehydration, isoelectric focusing was performed on an IPGphor II unit (Bio-Sciences Corp., Piscataway, NJ, USA) with the following parameters: 30 V for 12 h, 50 V for 1 h, 100 V for 1 h, 300 V for 1 h, 600 V for 1 h, 1000 V for 2 h, and 8000 V for 10 h. After isoelectric focusing, the strips were equilibrated in equilibration buffer [6 M urea, 2% SDS, 2.5 M Tris-HCl (pH 8.8), 30% glycerol, 0.002% (w/v) bromophenol blue and 65 M DTT] for 15 min. Then, the strips were equilibrated in alkylation buffer [6 M urea, 2% SDS, 2.5 M Tris-HCl (pH 8.8), 30% glycerol, 0.002% (w/v) bromophenol blue and 4% iodoacetamide (IAA)] for 15 min. The second dimension separation of proteins was run on SDS-PAGE gels (12.5% polyacrylamide, w/v) using an Ettan^{TM} Daltsix apparatus (GE Healthcare Bio-Sciences Corp., Piscataway, NJ, USA). Electrophoresis was carried out at 25°C and 2 W/gel for 45 min and then 13 W/gel for 4.5 h until the bromophenol blue dye front arrived at the bottom of the gels.

The gels were stained with Coomassie brilliant blue R-250. The proteins were visualized by Coomassie brilliant blue R250 staining, and gel images were acquired using an image scanner (GE Healthcare Bio-Sciences Corp., Piscataway, NJ, USA). Image analysis was performed with Image Master 2D Platinum software version 7.0 (GE Healthcare Bio-Sciences Corp., Piscataway, NJ, USA). Spots were considered reproducible when they were well resolved in the three biological replicates. Protein spots were selected for further analysis based on an abundance ratio ≥ 2 and a threshold of $p \leq 0.05$.

2.4 In-Gel Digestion and MALDI-TOF/TOF Analysis

Selected protein spots were manually excised from the 2-DE gels. The gel spots were washed twice. The gel spots were destained at room temperature for 30 min. Then, the destaining solution was removed, and dehydration solution 1 was added to the tube. After 30 min, dehydration solution 1 was removed, and dehydration solution 2 was added to the tube for 30 min. Then, dehydration solution 2 was removed, and 10 μL working solution was added to the tube. After 30 min, cover solution was added to the tube overnight (16 h) at 37°C. The mixture was centrifuged for 5 min at 37°C and the supernatants were transferred into another tube. The peptide extracts and the supernatant of the gel spot were combined and then completely dried.

The samples were resuspended in 5 μL 0.1% TFA followed by mixing in a 1:1 ratio with a matrix consisting of a saturated solution of α-cyano-4-hydroxy-trans-cinnamic acid in 50% ACN and 0.1% TFA. One 1 μL mixture was spotted on a stainless steel sample target plate. Peptide MS and MS/MS were performed on an ABI 5800 MALDI-TOF/TOF Plus Mass Spectrometer (Applied Biosystems, Foster City, USA). Data were acquired in a positive MS reflector using a CalMix5 standard to calibrate the instrument (ABI5800 Calibration Mixture). Both the MS and MS/MS data were integrated and processed using GPS Explorer V3.6 software (Applied Biosystems, USA) with default parameters. Based on combined MS and MS/MS spectra, proteins were successfully identified based on 95% or higher confidence intervals of

their scores in the MASCOT V2.3 search engine (Matrix Science Ltd., London, UK) using the following search parameters: NCBInr-Viridiplantae database; trypsinas the digestion enzyme; one missed cleavage site; fixed modifications of carbamidomethyl (C); partial modifications of acetyl (Protein N-term), deamidated (NQ), dioxidation (W), oxidation (M); 100 ppm for precursor ion tolerance and 0.3 Da for fragment ion tolerance.

2.5 Quantitative Real-Time PCR (qRT-PCR)

To investigate the relationship between the transcriptional and translational levels of inflorescence-development-related genes, we used qRT-PCR to analyze 10 genes based on the proteomics results (Supplemental Table S1). Total RNA was isolated using the method described by Schultz [15]. cDNA was synthesized from 1 μg of total RNA with PrimeScript reverse transcriptase (TaKaRa, Japan) according to the manufacturer's instructions. qRT-PCR was performed using SYBR Green Real-time PCR master mix (Toyobo, Japan) with an ABI 7500 real-time system (Applied Biosystems, Foster City, CA, USA). The 18S gene was used as a reference gene. The relative expression of the target genes was calculated using the comparative *Ct* method.

3 Results

3.1 Identification of Differentially Expressed Proteins in Different Inflorescence Types

To better understand the differences in inflorescence types of castor at different developmental stages, we carried out a comparative proteomic study (Fig. 1). A total of 72 differentially abundant protein spots (DAPs) were identified (Supplemental Table S2). Among them, 16 DAPs were identified at the 4 euphylla stages, 14 DAPs were identified at the 5 euphylla stages, 25 DAPs were identified at the primary stem heading stage, and 17 DAPs were identified at the second-level branching stage (Fig. 2). The 72 differentially expressed proteins in different castor inflorescences were heatmapped (Fig. 3 and Supplemental Table S3).

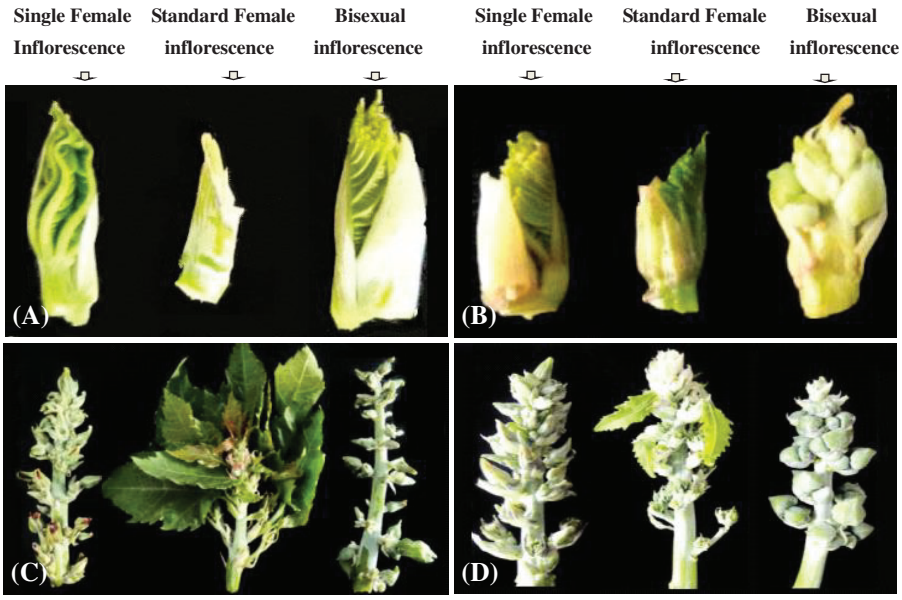

Figure 1: The morphology of inflorescence. (A) 4 euphylla stage; (B) 5 euphylla stage; (C) Main stem heading stage; (D) Second-level branching state

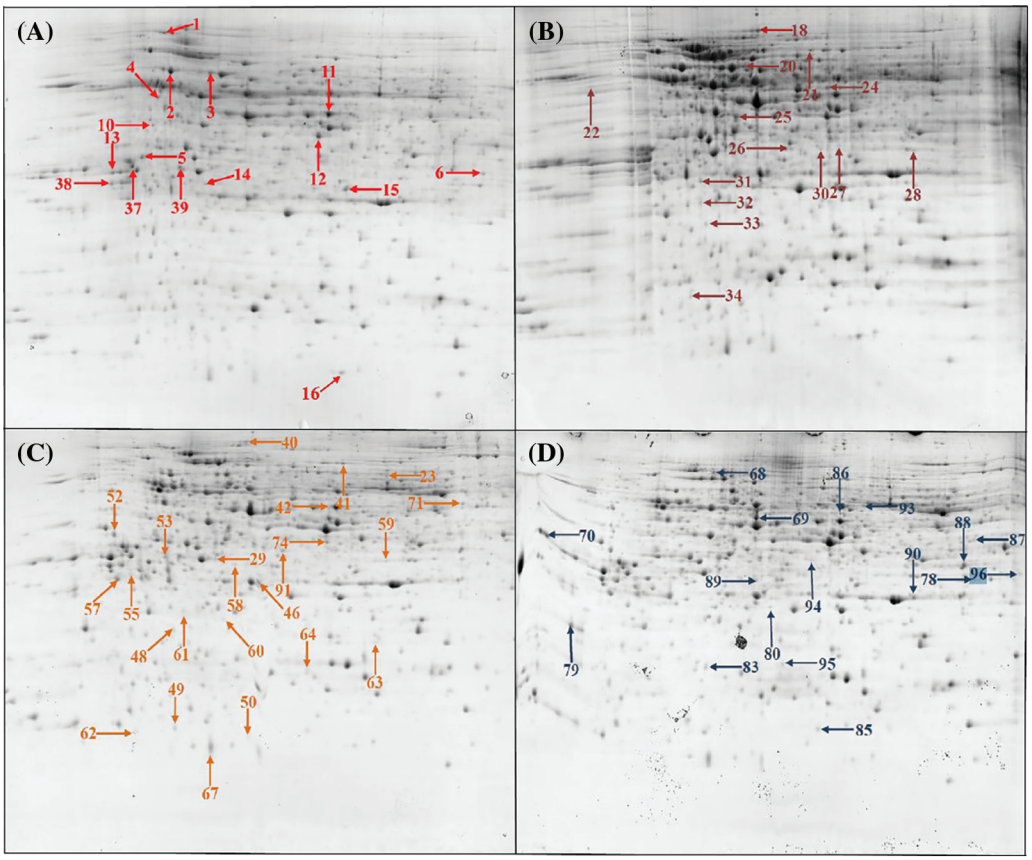

Figure 2: The two-dimensional electrophoresis of castor inflorescence proteins. (A) 4 euphylla stage; (B) 5 euphylla stage; (C) Main stem heading stage; (D) Second-level branching state

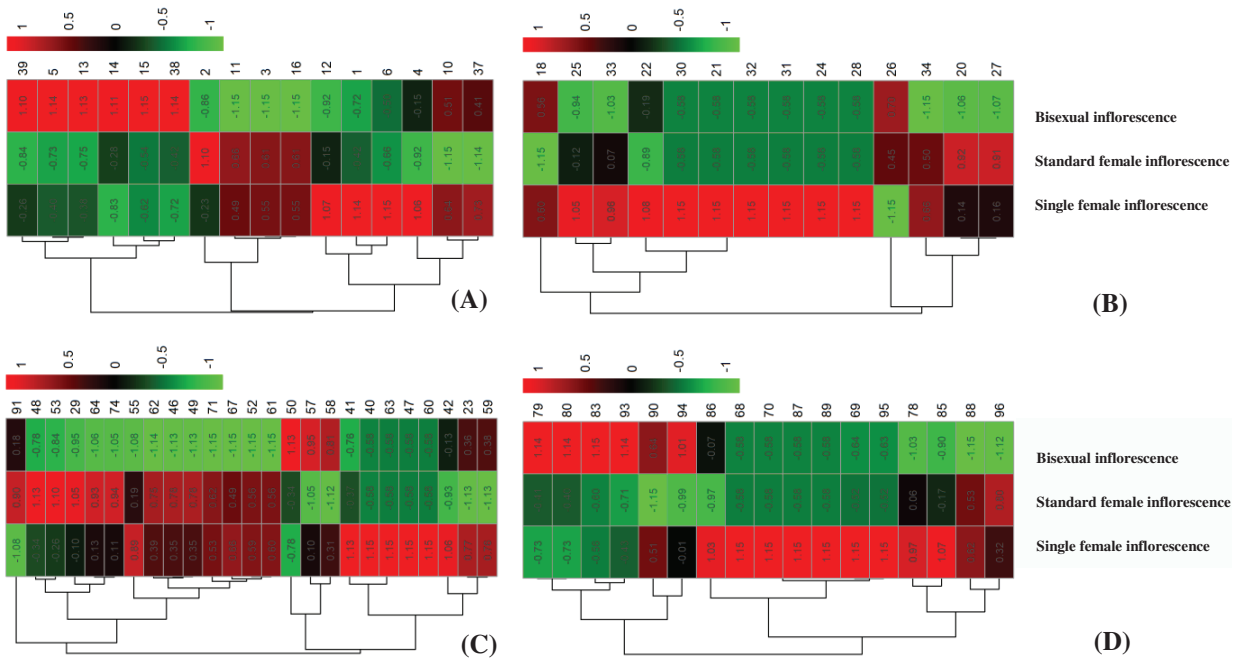

Figure 3: Hierarchical clustering of the 73 deferentially expressed proteins at different inflorescence development stage. (A) 4 euphylla stage; (B) 5 euphylla stage; (C) Main stem heading stage; (D) Second-level branching state

3.2 Functional Classification of Deferentially Expressed Proteins

We carried out GO annotation on 72 DAPs and divided them into 22 functional categories based on their biological functions (Fig. 4) and Supplemental Table S4). Of these, biological processes had 8 GO terms, cellular components had 8 GO terms, and molecular functions had 6 GO terms.

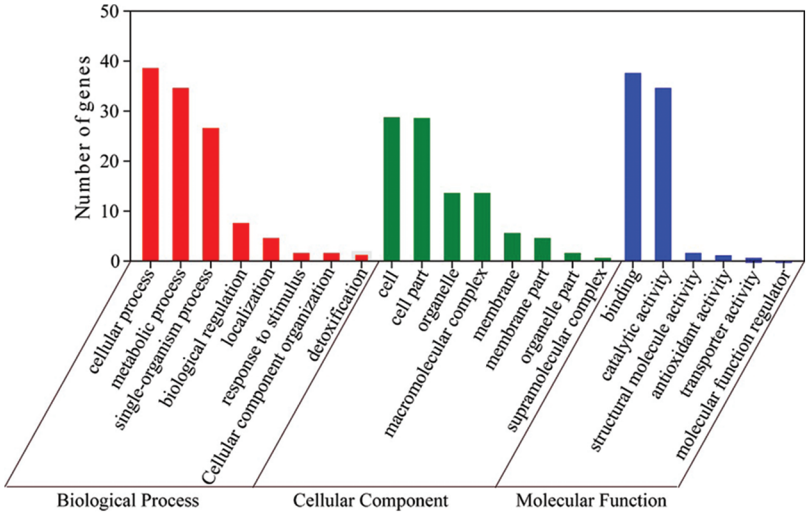

Figure 4: Biological process, cellular component and molecular function of the 72 identified proteins, respectively

All 72 DAPs were classified into 12 categories of Clusters of orthologous groups, of which the representative group was "energy production and conversion", followed by posttranslational modification, protein turnover, chaperons (13 DAPs) and unknown (13 DAPs) (Fig. 5 and Supplemental Table S5).

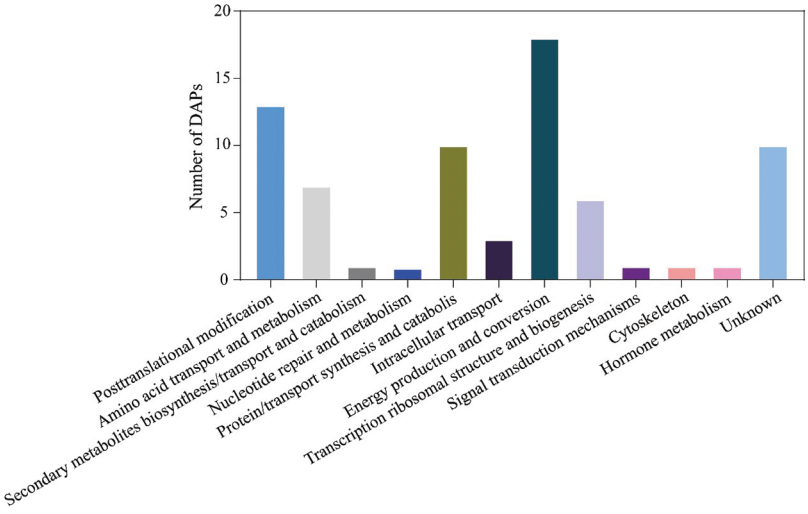

Figure 5: The functional category of DAPs identified by the 2-DE

To further explore the biological functions of these proteins, 72 DAPs were enriched in 30 pathways based on the KEGG database (Fig. 6 and Supplemental Table S6). These DAPs were significantly enriched in the following pathways: carbon metabolism, metabolic pathway, carbon fixation in photosynthetic organisms, biosynthesis of amino acids, proteasome, glycolysis/gluconeogenesis, and cysteine and methionine metabolism.

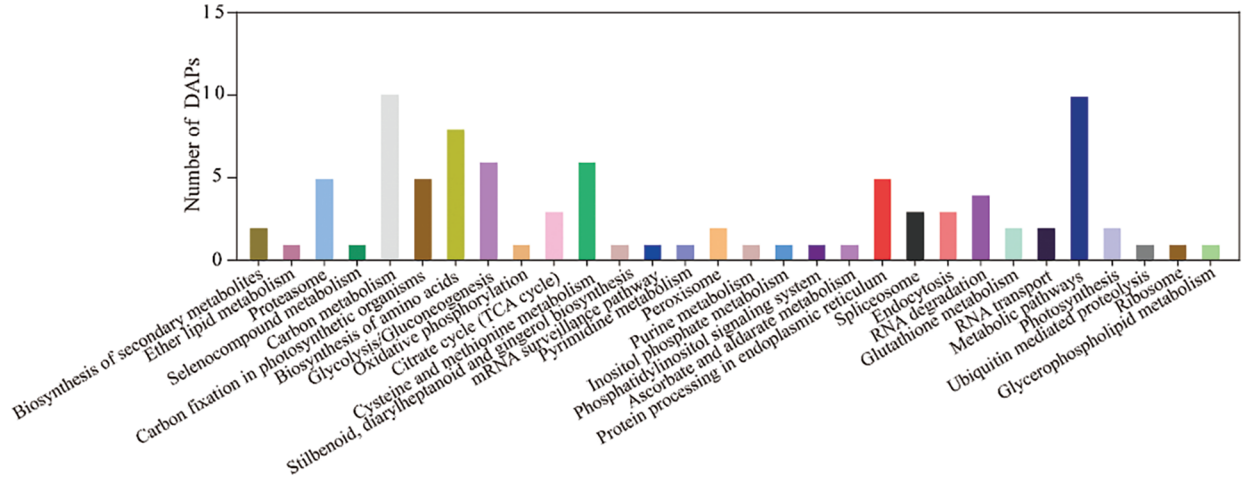

Figure 6: The functional category of DAPs identified by the 2-DE according to KEGG pathway

3.3 Validation of the Differentially Expressed Proteins

To assess the correlation between the abundance of DAPs and the transcript levels, ten DAPs were selected for qRT-PCR analyses. The results showed that the transcription and protein expression levels were consistent for 9 differentially expressed proteins in castor inflorescence (number of protein 1, 13, 23, 29, 41, 42, 71, 74, 91). However, the transcription and protein expression levels were not consistent with that of protein 58 in the main stem heading stage of castor inflorescence (Table 1).

Table 1: The comparison of expressed level between mRNA and protein of DAPs

No. of protein	Description	ZB/ZD ratio (Protein)	ZB/ZD qPCR ratio	Trends	ZL/ZD ratio (Protein)	ZL/ZD qPCR ratio	Trends
1	Heat shock protein	0.163 ± 0.117	0.804 ± 0.267	− −	0	0.585 ± 0.356	− −
13	14-3-3 protein	0.472 ± 0.118	0.891 ± 0.346	− −	3.146 ± 0.2249	1.094 ± 0.256	+ +
23	Enolase	0.718 ± 0.313	0.933 ± 0.346	− −	0.940 ± 0.2013	0.958 ± 0.242	− −
29	Inositol-1-monophosphatase	2.054 ± 0.113	1.257 ± 0.279	+ +	0.218 ± 0.0134	0.734 ± 0.156	− −
41	Phospholipase D alpha	0	0.624 ± 0.452	− −	0.509 ± 0.1209	0.740 ± 0.291	− −
42	Phosphoglycerate kinas	0	0.665 ± 0.273	− −	0.399 ± 0.1001	0.604 ± 0.372	− −

(Continued)

Table 1 (continued)

No. of protein	Description	ZB/ZD ratio (Protein)	ZB/ZD qPCR ratio	Trends	ZL/ZD ratio (Protein)	ZL/ZD qPCR ratio	Trends
58	Triosephosphate isomerase	0	0.699 ± 0.273	− −	0.134 ± 0.2133	1.028 ± 0.262	− +
71	Isocitrate dehydrogenase	1.053 ± 0.122	1.729 ± 0.163	+ +	0	0.482 ± 0.153	− −
74	Fructose-bisphosphate aldolase	1.272 ± 0.167	1.527 ± 0.245	+ +	0.622 ± 0.2132	0.797 ± 0.513	− −
91	Cysteine synthase	3.217 ± 0.101	2.085 ± 0.145	+ +	2.413 ± 0.2213	1.832 ± 0.214	+ +

Note: ZD, main stem heading stage of the SiFF; ZB, main stem heading stage of StFF; ZL, main stem heading stage of BF. +, up-regulated; −, down-regulated.

4 Discussion

The inflorescence style determines the crop yield [16,17]. The development of inflorescences is a complex process with many interactions, including the establishment of meristems and differences in expansion and division modes [18]. In this study, it was revealed that DAPs from castor inflorescence are primarily involved in carbon metabolism, amino acid metabolism, and protein biosynthesis. For example, DAPs are primarily involved in four carbon metabolic pathways (carbon metabolism, carbon fixation in photosynthetic organisms, the TCA cycle and glycolysis/gluconeogenesis). In addition, the observed DAPs involved in carbon metabolism including S-adenosylmethionine synthase (spot. 11), oxygen-evolving enhancer protein 1 (spot. 14), enolase (spot. 23), phosphoglyceratekinase (spot. 42), triosephosphateisomerase (spot. 58), isocitratedehydrogenase (spot. 71), fructose-bisphosphatealdolase (spot. 74), malatedehydrogenase (spot. 87) (Supplemental Table S2). Generally, carbohydrate metabolism is involved in regulating the developmental process from embryonic development to aging [19,20]. Carbohydrate metabolism also plays an important role in plant sexual reproduction as the sugar content determines flower formation and flower organ development [20,21]. In herbaceous plants, flowering represents the most energy-consuming step crucial for reproductive success, and photosynthesis in the inflorescence provides the carbon needed for reproduction. It is well known that the photosynthesis of plants is mainly performed by leaves, but the reproductive organs of some plants can also photosynthesize and fix a large amount of carbon. In previous studies, some changes in inflorescence photosynthesis during plant development have been reported. Previous studies have shown that the inflorescence can absorb and distribute carbon mainly in the vegetative organs during flower development [22]. However, the inflorescence is the primary source of carbon uptake, and it has an important function in nutritional balance by promoting leaf development, which in turn will ensure the availability of carbohydrates for flower development. Previous studies have also shown that carbohydrates not only ensure energy supply during flowering but also affect flower bud differentiation of inflorescence. For example, at the early inflorescence stages of oil palm, the vegetative to reproductive phase transition of the meristems was regulated by sugar balance. We also observed that proteins and metabolites assigned to carbon metabolism were deferentially expressed at the primary stem heading stage of inflorescence. Therefore, different inflorescences may primarily affect growth and development through differences in the distribution of imported carbohydrates and exported photoassimilates.

Eight DAPs involved in cysteine and methionine metabolism were induced at inflorescence development stages, which suggested that cysteine and methionine metabolism play critical roles in the regulation of inflorescence development in castor. In general, many plant cysteine-rich peptides with potential antimicrobial properties have been predicted [23]. At the same time, plants can defend against tolerant environmental stresses and plant pathogens by some proteins having plant-specific cysteine-rich motifs [24]. Additionally, the cysteine metabolism pathway has been implicated in diverse functions due to the cysteine protease interacting with FZP increasing the number of secondary inflorescence branches of rice [25]. GIP, a Petunia hybrida GA-induced cysteine-rich protein, had a possible role in the transition to flowering [26]. In addition, a cysteine proteinase inhibitor may also involve in the regulation of petal wilting in senescing carnation (*Dianthus caryophyllu*s L.) flowers [27]. The cysteine synthase (spot. 91) and cysteine proteinase inhibitor (spot. 91) for a SiFF at the main stem heading stage and second-level branching state showed were downregulated and upregulated, respectively. The uniform accumulation of this protein involved in cysteine metabolism might contribute to inflorescence differentiation.

The methionine for plants, as an amino acid, supports additional roles than simply serving as a building block for protein synthesis. This is because methionine is the immediate precursor of *S*-adenosylmethionine (AdoMet), which plays many key roles as the major methyl-group donor in transmethylation reactions and an intermediate in the biosynthesis of polyamines and of the phytohormone ethylene [28]. Additionally, the Met cycle is also a series of reactions catalyzing the recycling of the sulfur (S) compound 5′-methylthioadenosine (MTA) to Met. Phloem-specific reconstitution of Met cycle activity was sufficient to rescue their S-dependent mutant phenotypes. Accordingly, it was concluded from these analyses that phloem-specific S recycling during periods of S starvation is essential for the biosynthesis of polyamines required for flowering development [29]. For example, ectopic expression of soybean methionine synthase delays flowering time [30]. In the present study, the abundance of S-adenosylmethionine synthase (spot 11 and spot 42) showed different levels for different inflorescence styles at the 4 euphylla stage and main stem heading stage. This different accumulation of methionine might suggest that to speculate the function of Met in inflorescence development deserves further investigation.

Carbohydrate and energy metabolism play an important role in providing the necessary energy for plant inflorescence development. In addition, carbon metabolism can effectively connect other metabolic pathways. Generally, the glycolytic pathway (EMP) is a main driving force during plant growth and development processes because it can produce energy and cell component precursors [31]. This pathway refers to the nonoxidative pathway, which is catalyzed by several key enzymes such as malate dehydrogenase, triosephosphate isomerase and phosphoglycerate kinase. It was revealed that the *MDH* gene from Chinese cabbage was overexpressed in inflorescence apical meristems, which resulted in taller inflorescence stems of transgenic *Arabidopsis* lines [32]. Numerous studies regarding the function of some genes in the EMP pathway during inflorescence development have been reported [33]. For example, the efficient EMP pathway was beneficial for the flower bud development of grape, which can provide material and energy for each spike inflorescence primordium further to the development of the second-level inflorescence axis. EMP activation is crucial and associated with bud dormancy transition in tree peony [33]. In this study, the levels of 10 DAPs involved in carbon metabolism changed at inflorescence development stages (Supplemental Table S5).

5 Conclusions

The structure of castor inflorescences directly affects the yield of castor, but until now, little research has been performed on the three castor inflorescence types for their complex structure. In this study, three inflorescence types at different developmental stages were analyzed using proteomic approach, resulting in the identification of 72 DAPs. The primary metabolic pathways involved in DAPs included carbon metabolism and energy metabolism.

Acknowledgement: Thanks to AJE for providing editing services to the paper.

Funding Statement: This study was supported by the National Natural Science Foundation of China (31860071); Research and Reform Practice Project in New Agricultural Sciences of the Ministry of Education in 2020 (2020114); Natural Science Foundation of Inner Mongolia Autonomous Region (2021MS03008); Inner Mongolia Autonomous Region Grassland Talents Innovation Team—Castor Molecular Breeding Research Innovative Talent Team Rolling Support Project (2022); Higher Education Teaching Reform Research Project of National Ethnic Affairs Commission in 2021 (21082); Fundamental Research Funds in Higher Education Institutions of Inner Mongolia in 2022 (237); Autonomous Region Basic Scientific Reasearch Business Fee Projest of Inner Mongolia MinZu University in 2023 (225, 227, 244); Inner Mongolia Autonomous Region Castor Industry Collaborative Innovation Center Construction Project (MDK2021011, MDK2022014); Open Fund Project in State Key Laboratory of Castor Breeding of China's National Ethnic Affairs Commission (MDK2021008); and Science and Technology Research Project of Jilin Provincial Department of Education (JJKH20220010KJ).

Author Contributions: Fenglan Huang designed the experiments; Xue Lei and Yong Zhao performed the experiments, wrote the manuscript, critically revised the draft and updated the manuscript for publication. Rui Luo, Mingda Yin, Yanpeng Wen, Zhiyan Wang and Xuemei Hu performed data analysis. All authors have read and agreed to the published version of the manuscript.

Conflicts of Interest: The authors declare that they have no conflicts of interest to report regarding the present study.

References

1. Anjani, K. (2012). Castor genetic resources: A primary gene pool for exploitation. *Industrial Crops & Products, 35(1),* 1–14.
2. Patel, J. K., Patel, P. C. (2014). Genetic variability, heritability and genetic advance for yield and yield components in castor (*Ricinus communis* L.) genotypes. *International Journal of Plant Sciences, 9,* 385–388.
3. Shifriss, O. (1960). Conventional and unconventional systems controlling sex variations in Ricinus. *Journal of Genetics, 57(2–3),* 361–388.
4. George, W. L., Shifriss, O. (1967). Interspersed sexuality in ricinus. *Genetics, 57(2),* 347.
5. Jakob, K. M., Dan, A. (1956). Sex inheritance in *Ricinus communis* L.: Evidence for a genetic change during the ontogeny of female sex reversals. *Genetica, 36(3),* 253–259.
6. Shifriss, O. (1965). Sex instability in ricinus. *Genetics, 41(2),* 265–280.
7. Wang, Y., Wang, J., Lai, L., Jiang, L., Zhuang, P. et al. (2014). Geographic variation in seed traits within and among forty-two species of *Rhododendron* (Ericaceae) on the Tibetan plateau: Relationships with altitude, habitat, plant height, and phylogeny. *Ecology & Evolution, 4(10),* 1913–1923.
8. Khryanin, V. N. (2007). Evolution of the pathways of sex differentiation in plants. *Russian Journal of Plant Physiology, 54(6),* 845–852.
9. Solanki, S. S., Joshi, P. (2000). Stability parameters for sex expression in castor (*Ricinus communis* L.). *Journal of Oilseeds Research, 17(2),* 242–248.
10. Parvathy, S. T., Prabakaran, A. J., Jayakrishna, T. (2021). Probing the floral developmental stages, bisexuality and sex reversions in castor (*Ricinus communis* L.). *Scientific Reports, 11(1),* 4246.
11. Anjani, K. (2012). Castor genetic resources: A primary gene pool for exploitation. *Industrial Crops & Products, 35(1),* 1–14. https://doi.org/10.1016/j.indcrop.2011.06.011
12. Zimmerman, L. H., Smith, J. D. (1966). Production of F1 hybrid seed in castorbeans by use of sex genes sensitive to environment. *Crop Science, 6(5),* 406–409. https://doi.org/10.2135/cropsci1966.0011183X000600050005x

13. Tan, M., Xue, J., Wang, L., Huang, J., Fu, C. et al. (2015). Transcriptomic analysis for different sex types of *Ricinus communis* L. during development from apical buds to inflorescences by digital gene expression profiling. *Frontiers in Plant Science, 6,* 1208.
14. Granier, F. (2010). Extraction of plant proteins for two-dimensional electrophoresis. *Electrophoresis, 9(11),* 712–718. https://doi.org/10.1002/(ISSN)1522-2683
15. Schultz, D. J., Craig, R., Cox-Foster, D. L., Mumma, R. O., Medford, J. I. (1994). RNA isolation from recalcitrant plant tissue. *Plant Molecular Biology Reporter, 12(4),* 310–316. https://doi.org/10.1007/BF02669273
16. Harder, L. D., Jordan, C. Y., Gross, W. E., Routley, M. B. (2004). Beyond floricentrism: The pollination function of inflorescences. *Plant Species Biology, 19(3),* 137–148. https://doi.org/10.1111/j.1442-1984.2004.00110.x
17. Wyatt, R. (1982). Inflorescence architecture: How flower number, arrangement, and phenology affect pollination and fruit-set. *American Journal of Botany, 69(4),* 585–594. https://doi.org/10.1002/j.1537-2197.1982.tb13295.x
18. Bartlett, M. E., Thompson, B. (2014). Meristem identity and phyllotaxis in inflorescence development. *Frontiers in Plant Science, 5(250),* 508. https://doi.org/10.3389/fpls.2014.00508
19. Gibson, S. I. (2005). Control of plant development and gene expression by sugar signaling. *Current Opinion in Plant Biology, 8(1),* 93–102. https://doi.org/10.1016/j.pbi.2004.11.003
20. Rolland, F., Baena-Gonzalez, E., Sheen, J. (2006). Sugar sensing and signaling in plants: Conserved and novel mechanisms. *Annual Review of Plant Biology, 57(1),* 675–709. https://doi.org/10.1146/annurev.arplant.57.032905.105441
21. Sawicki, M., Jacquens, L., Baillieul, F., Clement, C., Vaillant-Gaveau, N. et al. (2015). Distinct regulation in inflorescence carbohydrate metabolism according to grapevine cultivars during floral development. *Physiologia Plantarum, 154(3),* 447–467. https://doi.org/10.1111/ppl.12321
22. Vaillant-Gaveau, N., Maillard, P., Wojnarowiez, G., Gross, P., Clément, C. et al. (2011). Inflorescence of grapevine (*Vitis vinifera* L.): A high ability to distribute its own assimilates. *Journal of Experimental Botany, 62(12),* 4183.
23. Maróti, G., Downie, J. A., Kondorosi, É. (2015). Plant cysteine-rich peptides that inhibit pathogen growth and control rhizobial differentiation in legume nodules. *Current Opinion in Plant Biology, 26,* 57–63.
24. Miyakawa, T., Hatano, K., Miyauchi, Y., Suwa, Y., Sawano, Y. et al. (2014). A secreted protein with plant-specific cysteine-rich motif functions as a mannose-binding lectin that exhibits antifungal activity. *Plant Physiology, 166(2),* 766–778.
25. Huang, Y., Zhao, S., Fu, Y., Sun, H., Ma, X. et al. (2018). Variation in the regulatory region of FZP causes increases in secondary inflorescence branching and grain yield in rice domestication. *The Plant Journal, 96(4),* 716–733.
26. Ben-Nissan, G., Lee, J. Y., Borohov, A., Weiss, D. (2010). GIP, a Petunia hybrida GA-induced cysteine-rich protein: A possible role in shoot elongation and transition to flowering. *The Plant Journal, 37(2),* 229–238.
27. Hiroaki, S., Kenichi, S., Toshihito, Y., Teruyoshi, H., Shigeru, S. (2002). Is a cysteine proteinase inhibitor involved in the regulation of petal wilting in senescing carnation (*Dianthus caryophyllus* L.) flowers? *Journal of Experimental Botany, 53(368),* 407–413.
28. Ravanel, S., Gakiere, B., Job, D., Douce, R. (1998). The specific features of methionine biosynthesis and metabolism in plants. *Proceedings of the National Academy of Sciences, 95(13),* 7805–7812.
29. Zierer, W., Hajirezaei, M. R., Kai, E., Sauer, N., Pommerrenig, B. (2015). Phloem-specific methionine recycling fuels polyamine biosynthesis in a sulfur-dependent manner and promotes flower and seed development. *Plant Physiology, 170(2),* 790–806.
30. Sha, A. H., Gao, Z. L., Wu, H., Lin, D. Z., Zhang, Q. L. et al. (2015). Ectopic expression of soybean methionine synthase delays flowering time in transgenic tobacco plants. *Biologia Plantarum, 59(1),* 47–54.
31. Jojima, T., Inui, M. (2015). Engineering the glycolytic pathway: A potential approach for improvement of biocatalyst performance. *Bioengineered Bugs, 6(6),* 328–334.
32. Li, Q. F., Jing, Z., Zhang, J., Dai, Z. H., Zhang, L. G. (2016). Ectopic expression of the Chinese cabbage malate dehydrogenase gene promotes growth and aluminum resistance in *Arabidopsis*. *Frontiers in Plant Science, 7,* 1180.
33. Wang, H., Wang, X., Zhao, J., Shi, X., Xiaohao, J. I. et al. (2017). The influence of changes of respiratory metabolism in bud on grapes flower buds differentiation in greenhouse. *China Fruits, 4,* 5–10.

Appendix

Table S1: The primer sequences for Real-Time PCR

Table S2: The information of identification of differential proteins in *Ricinus communis* L. inflorescences by mass spectrometry (MS) analysis

Table S3: The expressed level of differential proteins in *Ricinus communis* L. inflorescences by mass spectrometry (MS) analysis

Table S4: Gene Ontology (GO) functional annotation of DAPs

Table S5: Bioinformatics analysis of differential abundance protein species (DAPS) identified by two-dimensional electrophoresis (2-DE)

Table S6: The analysis of differential abundance protein species (DAPS) identified by two-dimensional electrophoresis (2-DE) KEGG pathways of DAPS